Trajectory Control of Mars Rover Based on Fuzzy Control Theory

Caiying Yang, Yuesheng Ye, Qingnan Huang, Ziying Zeng, Hongyang Zhang

***Abstract*—A variable-parameter fuzzy model for the Mars Rover is designed to account for time-varying systems and sector nonlinearities. This model addresses the limitations of the traditional T-S fuzzy model by increasing the number of fuzzy rules, which allows for a more accurate representation of the Mars Rovers dynamics. Furthermore, the model reduces complexity through linearization, making it more practical for control system design. Gain-scheduling controllers for the Mars Rover is designed based on the second-order Lyapunov stability theorem. This approach ensures that the controller provides stable and reliable performance for the Rover under varying operating conditions. We will demonstrate the effectiveness of our work by simulation, showcasing the superiority over traditional methods. This variable-parameter fuzzy model has the potential to enhance the performance and reliability of the Mars Rover in real-world applications.**

***Index Terms*—FPV systems, Sector nonlinearity, Second-order Lyapunov stability theorem, Gain-scheduling controllers.**

I. Introduction

MARS landing mission[1, 2] is divided into entry phase, descent phase and landing phase, and the realization of each phase of the mission brings great challenges to system engineering. Although Viking-1 and Viking-2 successfully landed on the surface of Mars on July 20th, 1976 and September 3rd, 1976 respectively[3], they didn't control their trajectories when they entered the atmosphere of Mars. However, the precise control of this stage is very important for the subsequent spacecraft landing process, whether it is the reentry stage of the return capsule returning to Earth or the entry stage of the probe entering the Martian atmosphere. When the Mars probe enters the Martian atmosphere, on the one hand, due to the incomplete information about the Martian atmosphere and the unstable state of the Martian atmosphere, it is often accompanied by strong winds and sandstorms, which brings great challenges for the Mars probe to reach the parachute opening smoothly. On the other hand, Mars is far away from the earth, which makes the delay time of information transmission between Mars and the earth about 10 minutes, while the whole process of entering the segment is only about 7 minutes, which brings great difficulties for ground controllers to control the Mars probe in real time. Therefore, it is of great significance to study an adaptive controller that can be used in the entry section of Mars probe to realize the dream of deep space exploration.

Fuzzy control theory offers a promising approach to address these challenges. However, existing research on fuzzy systems has mainly focused on systems with a limited number of linear time-invariant subsystems, which may not adequately capture the time-varying nature of the Martian environment. If we consider the time-varying characteristics of the system, it will inevitably lead to the problem of rule explosion[4]. Additionally, the fuzzy T-S model provides only an approximate description of the initial nonlinear dynamics, which can be more conservative when incorporating time-varying parameters. Finding a balance between accuracy and complexity in dynamic modeling is crucial to ensure the success of Mars missions.

Trajectory control plays an important role in the entry phrase. Over the years, several pseudo-spectral methods[5], such as the Legendre pseudo-spectral method[6], Radau pseudo-spectral method[7], and Gauss pseudo-spectral method[8], have been developed and utilized for trajectory control problems. However, these methods often rely heavily on the designers experience, and there is no clear rule for fixed node selection, which can limit their effectiveness. In recent research, significant advancements have been made in trajectory optimization for Mars entry. In 2011, Li et al.[9] presented a trajectory optimisation method based on desensitised optimal control and non-linear direct constructive programming. This method integrated considerations of uncertainties in aerodynamic parameters and trajectory tracking performance, reducing the difficulty of tracking guidance. Additionally, TSMC[10] has been proposed for tracking a reference trajectory. Subsequent studies by researchers like J. Dai[11] and L. Long[12] have further refined this line of study, offering new insights and improvements. In 2018, V. Saranya[13] proposed a controller based on dynamic inverse design to track the reference state trajectory, then an adaptive neural network PID controller[14] is proposed in the next year. The advancements in trajectory planning and guidance methods demonstrate the ongoing efforts to improve the accuracy and reliability of Mars atmospheric entry, which is vital for the success of future Mars missions.

The proposed solution to the modeling problem involves constructing a variable-parameter model using sector nonlinearity[15]. This approach is crucial in practical applications as it reduces the fuzzy rules, simplifying the analysis and design of the control system. Our primary work is to incorporate time-varying parameters into traditional T-S

Manuscript received September 22, 2023; revised February 9, 2024.

This work was supported by Funds of National Science of China under Grant 11901116.

Caiying Yang is an undergraduate student of the School of Mathematics and Systems Science, Guangdong Polytechnic Normal University, Guangzhou 510665, P. R. China. (Email: 2521035483@qq.com).

Yuesheng Ye is an undergraduate student of the School of Mathematics and Systems Science, Guangdong Polytechnic Normal University, Guangzhou 510665, P. R. China. (Email: 3406149630@qq.com).

Qingnan Huang is an undergraduate student of the School of Mathematics and Systems Science, Guangdong Polytechnic Normal University, Guangzhou 510665, P. R. China. (Email: 3280296322@qq.com).

Ziying Zeng is an undergraduate student of the School of Mathematics and Systems Science, Guangdong Polytechnic Normal University, Guangzhou 510665, P. R. China. (Email: 1516521147@qq.com).

Hongyang Zhang a lecturer of the School of Mathematics and Systems Science, Guangdong Polytechnic Normal University, Guangzhou 510665, P. R. China. (Corresponding author; Phone: 86-15004677167; Email: zhanghongyang@gpnu.edu.cn).

TABLE I
ACCOUNT FOR MODEL 1

ρ	Atmospheric Density
v	Flying Speed
γ	Trajectory Angle
m	Quality of Aircraft
ϕ	Bank Angle
s	Reference Area
C_D	Drag Coefficient
C_L	Lift Coefficient
r	Distance from the Center of Mars

fuzzy models using sector nonlinearity, which can otherwise lead to a rapid increase of fuzzy rules and system complexity. Our study focuses on modeling a exact dynamics of Martian inputs and designing gain scheduling controllers for the Mars rover. A full state feedback and a dynamic feedback output controller will be designed according to the model established before. By adopting this approach, the aim is to develop more accurate and efficient control systems for the Mars rover, addressing the specific challenges posed by the Martian environment and ensuring that the rover can navigate and operate effectively during entry, descent, and landing phases. These advancements have the potential to significantly improve the performance and reliability of Mars missions.

The main route of this paper is to establish an accurate kinetic model first, then analyze the stability by Quadratic Lia's stability theory to obtain the equivalent conditions of system stability, then design the controller for the model, and finally verify the scientific nature by simulation with MATLAB.

II. MODELING

A A Kinetic Model

Hongying Xu et al. proposed a dynamic model for the Mars' entry section in 2015[16]. We simplified the model and re-established a kinetic model of the entry phase taking into account the time-varying nature.

$$\begin{cases} \dot{r} = v\sin\gamma, \\ \dot{v} = -\dfrac{D^*}{\mathrm{m}} - \mathrm{g}\sin\gamma, \\ \dot{\gamma} = \dfrac{L^*}{\mathrm{m}v}\cos\phi - \left(\dfrac{\mathrm{g}}{v} - \dfrac{v}{r}\right)\cos\gamma, \\ D^* = \frac{C_D s\rho v^2}{2} \\ L^* = \frac{C_L s\rho v^2}{2} \end{cases} \tag{1}$$

Considering the reality, the drag parameters and aerodynamic parameters should be adjusted on-line in real time. However, the distance between Mars and the Earth is so far that there is a time error in information transmission. We set these two parameters unchanged during the simulation.

B F-P-V-Model

Due to the low degree of human understanding of Mars atmospheric information, and the great uncertainty of various parameters in the actual flight process, the variable

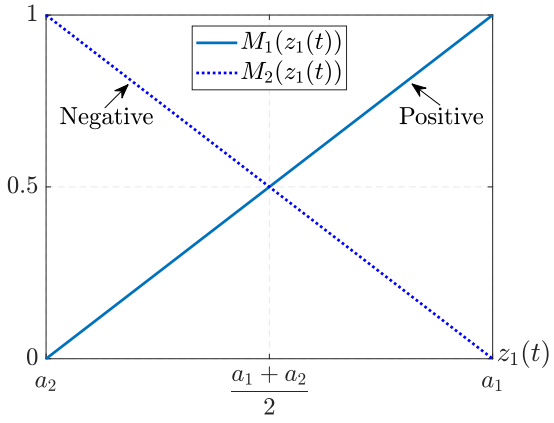

Fig. 1. Membership Functions of z_1

characteristics should be taken into account in the kinetic model of Mars probe. In 2018, Professor Ban Xiaojun's team[17] proposed a new nonlinear system called fuzzy variable parameter system, which fully considered the time-varying characteristics of the system. This provides a way of thinking for our modeling. We try to establish a kinetic model using the method of fuzzy division. Define model (1) as follows :

$$x_1 = \frac{r}{\mathrm{r}_0}, \quad x_2 = \frac{v}{\sqrt{\mathrm{g}\mathrm{r}_0}}, \quad x_3 = \gamma,$$
$$D = \frac{D^*(v,\rho)}{x_2\mathrm{mg}}, \quad L = \frac{L^*(v,\rho)}{x_2\mathrm{mg}}, \quad u = \cos\phi.$$

And the model will be as:

$$\begin{cases} \dot{x}_1 = x_2\sin x_3, \\ \dot{x}_2 = -Dx_2 - \sin x_3, \\ \dot{x}_3 = Lu - \frac{x_1 - x_2^2}{x_1^2 x_2}\cos x_3 x_1, \end{cases} \tag{2}$$

define:

$$z_1 = \sin x_3, \quad z_2 = \sin x_3, \quad z_3 = \frac{x_1 - x_2^2}{x_1^2 x_2}\cos x_3,$$

where $x_1 \in (r_1, r_2), x_2 \in (v_1, v_2), x_3 \in (-\alpha, \alpha), (0 \le \alpha < \frac{\pi}{2})$. Then model(2) can be written as:

$$\begin{cases} \dot{x}_1 = z_1 x_2, \\ \dot{x}_2 = -Dx_2 - z_2, \\ \dot{x}_3 = Lu - z_3 x_1. \end{cases} \tag{3}$$

Division $z_1 \sim z_3$ using sector nonlinearity. Since $\max z_1 = a_1$ and $\min z_1 = a_2$,

$$\begin{cases} z_1 = \sum_{l=1}^{2} M_l(z_1)a_l, \\ M_1(z_1) + M_2(z_1) = 1, \\ M_1(z_1) = \frac{z_1 - a_2}{a_1 - a_2}, \\ M_2(z_1) = \frac{a_1 - z_1}{a_1 - a_2}. \end{cases} \tag{4}$$

The membership function can be seen intuitively in Fig.1.

$z_2 = \sin x_3$ and its local sector can be seen in Fig.2, and the sector $[b_2, b_1]$ is formed by the attack of two lines $b_1 x_3$ and $b_2 x_3$.

$$\begin{cases} z_2 = \sum_{m=1}^{2} N_m(z_2)b_m x_3, \\ N_1(z_2) + N_2(z_2) = 1. \end{cases} \tag{5}$$

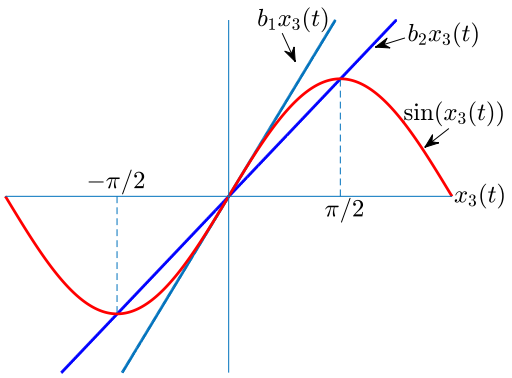

Fig. 2. z_1 and its Sector

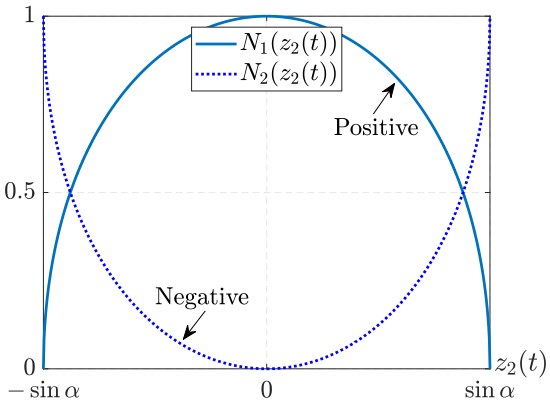

Fig. 3. Membership Functions of z_2

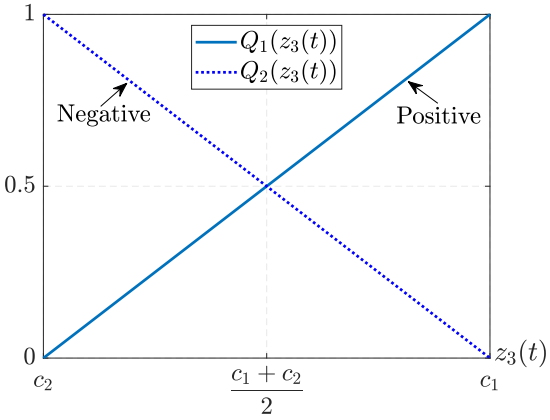

Fig. 4. Membership Functions of z_3

The membership function is:

$$N_1(z_2) = \begin{cases} 1, & z_2 = 0, \\ \dfrac{z_2 - b_2 \arcsin(z_2)}{(b_1 - b_2)\arcsin(z_2)}, & \text{otherwise}, \end{cases}$$

$$N_2(z_2) = \begin{cases} 0, & z_2 = 0, \\ \dfrac{b_1 arcsin(z_2) - z_2}{(b_1 - b_2) arcsin(z_2)}, & \text{otherwise}. \end{cases}$$

Considering z_3, since $\max z_3 = c_1$ and $\min z_3 = c_2$, we replace z_3 as before.

$$\begin{cases} z_3 = \sum\limits_{n=1}^{2} Q_n(z_3)c_n, \\ Q_1(z_3) + Q_2(z_3) = 1, \\ Q_1(z_3) = \dfrac{z_3 - c_2}{c_1 - c_2} \\ Q_2(z_3) = \dfrac{c_1 - z_3}{c_1 - c_2}. \end{cases} \tag{6}$$

The membership function can be seen intuitively in Fig.4.

According to (4) $\sim$ (6), the Fuzzy-Variable-Parameter Model (F-P-V-Model)for Mars Rover can be established.

$$\begin{cases} \dot{x} = \sum_{i=1}^{8} h_i(z)(A_i(\rho)x + B_i(\rho)u), \\ y = \sum_{i=1}^{8} h_i(z)(C_i(\rho)x + D_i(\rho)u), \end{cases} \tag{7}$$

The F-P-V-Model(7) has the following 8 rules:

Rule 1:

If z_1 is "Positive" , z_2 is "Positive" and z_3 is "Positive", then

$$\begin{cases} \dot{x} = A_1(\rho)x + B_1(\rho)u, \\ y = C_1(\rho)x + D_1(\rho)u. \end{cases}$$

Rule 2:

If z_1 is "Positive" z_2 is "Positive" and z_3 is "Negative", then

$$\begin{cases} \dot{x} = A_2(\rho)x + B_2(\rho)u, \\ y = C_2(\rho)x + D_2(\rho)u. \end{cases}$$

Rule 3:

If z_1 is "Positive" , z_2 is "Negative" and z_3 is "Positive", then

$$\begin{cases} \dot{x} = A_3(\rho)x + B_3(\rho)u, \\ y = C_3(\rho)x + D_3(\rho)u. \end{cases}$$

Rule 4:

If z_1 is "Positive" , z_2 is "Negative" and z_3 is "Negative" , then

$$\begin{cases} \dot{x} = A_4(\rho)x + B_4(\rho)u, \\ y = C_4(\rho)x + D_4(\rho)u. \end{cases}$$

Rule 5:

If z_1 is "Negative" , z_2 is "Positive" and z_3 is "Positive" , then

$$\begin{cases} \dot{x} = A_5(\rho)x + B_5(\rho)u, \\ y = C_5(\rho)x + D_5(\rho)u. \end{cases}$$

Rule 6:

If z_1 is "Negative" , z_2 is "Positive" and z_3 is "Negative" , then

$$\begin{cases} \dot{x} = A_6(\rho)x + B_6(\rho)u, \\ y = C_6(\rho)x + D_6(\rho)u. \end{cases}$$

Rule 7:

If z_1 is "Negative" , z_2 is "Negative" and z_3 is "Positive" , then

$$\begin{cases} \dot{x} = A_7(\rho)x + B_7(\rho)u, \\ y = C_7(\rho)x + D_7(\rho)u. \end{cases}$$

Rule 8:

If z_1 is "Negative" , z_2 is "Negative" and z_3 is "Negative" , then

$$\begin{cases} \dot{x} = A_8(\rho)x + B_8(\rho)u, \\ y = C_8(\rho)x + D_8(\rho)u. \end{cases}$$

Where, z_1, z_2, z_3 are premise variables,

$$A_1(\rho) = A_{111}(\rho) = \begin{bmatrix} 0 & a_1 & 0 \\ 0 & -D(\rho) & -b_1 \\ -c_1 & 0 & 0 \end{bmatrix}$$

$$A_2(\rho) = A_{112}(\rho) = \begin{bmatrix} 0 & a_1 & 0 \\ 0 & -D(\rho) & -b_1 \\ -c_2 & 0 & 0 \end{bmatrix}$$

$$A_3(\rho) = A_{121}(\rho) = \begin{bmatrix} 0 & a_1 & 0 \\ 0 & -D(\rho) & -b_2 \\ -c_1 & 0 & 0 \end{bmatrix}$$

$$A_4(\rho) = A_{122}(\rho) = \begin{bmatrix} 0 & a_1 & 0 \\ 0 & -D(\rho) & -b_2 \\ -c_2 & 0 & 0 \end{bmatrix}$$

$$A_5(\rho) = A_{211}(\rho) = \begin{bmatrix} 0 & a_2 & 0 \\ 0 & -D(\rho) & -b_1 \\ -c_1 & 0 & 0 \end{bmatrix}$$

$$A_6(\rho) = A_{212}(\rho) = \begin{bmatrix} 0 & a_2 & 0 \\ 0 & -D(\rho) & -b_1 \\ -c_2 & 0 & 0 \end{bmatrix}$$

$$A_7(\rho) = A_{221}(\rho) = \begin{bmatrix} 0 & a_2 & 0 \\ 0 & -D(\rho) & -b_2 \\ -c_1 & 0 & 0 \end{bmatrix}$$

$$A_8(\rho) = A_{222}(\rho) = \begin{bmatrix} 0 & a_2 & 0 \\ 0 & -D(\rho) & -b_2 \\ -c_2 & 0 & 0 \end{bmatrix}.$$

$$B_1(\rho) = B_2(\rho) = \ldots = B_8(\rho) = \begin{bmatrix} 0 \\ 0 \\ L(\rho) \end{bmatrix}.$$

When considering the evaluation output of the system, the universal form of F-P-V-Model (7) is as follow:

$$\begin{cases} \dot{x} = \sum_{i=1}^{8} h_i(z) \left(A_i(\rho)x + B_i^d(\rho)d + B_i^u(\rho)u \right), \\ e = \sum_{i=1}^{8} h_i(z) \left(C_i^e(\rho)x + D_i^{ed}(\rho)d + D_i^{eu}(\rho)u \right), \\ y = \sum_{i=1}^{8} h_i(z) \left(C_i^y(\rho)x + D_i^{yd}(\rho)d \right), \end{cases} \tag{8}$$

Atmospheric density is selected as a time-varying parameter in the F-P-V-Model established above, and fully considers the real environment when the detector works, which makes the simulation process more realistic. On the other hand, the sector nonlinearity is used for fuzzy division, which greatly reduces the complexity of the model and makes the simulation process easier to realize.

III. Stability Analysis

Martin Corless[18] proved the equivalence condition for the systems' stability by using quadratic Lyapunov theory. These conditions are all given in the form of matrix multiplication. In this section, we will also refer to this idea and give the equivalence condition to prove the stability of the system.

Considering the following continuous open-loop system, we have the theorem.

$$\dot{x} = \sum_{i=1}^{8} h_i(z) A_i(\rho) x. \tag{9}$$

Theorem 1: If a positive definite matrix P could be found, (9) is globally asymptotically stable.for each $\rho \in \Omega$, the following matrix inequalities are all true.

$$A_i^T(\rho)P + PA_i(\rho) < 0, i = 1, 2, ..., 8, \tag{10}$$

that is, P satisfies every matrix inequality.

Proof: Take the quadratic Lyapunov function candidate $V(x) = x^T P x$ and directly compute the derivative with respect to the time along the system (9)

$$\begin{aligned} \frac{\mathrm{d}V(x)}{\mathrm{d}t} &= \dot{x}^T P x + x^T P \dot{x} \\ &= \left(\sum_{i=1}^{8} h_i(z) A_i(\rho) x \right)^T P x + x^T P \sum_{i=1}^{8} h_i(z) A_i(\rho) x \\ &= \sum_{i=1}^{8} h_i(z) \left(x^T A_i^T(\rho) P x + x^T P A_i(\rho) x \right) \\ &= \sum_{i=1}^{8} h_i(z) x^T \left(A_i^T(\rho) P + P A_i(\rho) \right) x. \end{aligned}$$

As the membership functions are nonnegative and at least one is greater than zero, when (10) is satisfied, we have $\dot{V}(x) < 0$. Then (9) is globally asymptotically stable at the origin. ■

Inequality (10) contains infinitely linear matrix inequalities. Efficient convex optimization techniques are available to solve linear matrix inequalities. With this idea, the system of F-P-V with 16 linear matrix inequalities is available. This theory offers a promising approach to effectively tackle the complexities and uncertainties associated with the Martian atmospheric environment, potentially enhancing the practical application of stability analysis in this context.

IV. Controller Design

A Full-State-Feedback-Controller

F-P-V-Model (8) has the following form if substitute y into other variables.

$$\begin{cases} \dot{x} = \sum_{i=1}^{8} h_i(z)[A_i(\rho)x + B_i^d(\rho)d + B_i^u(\rho)u], \\ e = \sum_{i=1}^{8} h_i(z)[C_i^e(\rho)x + D_i^{ed}(\rho)d + D_i^{eu}(\rho)u]. \end{cases} \tag{11}$$

And $A_i(\rho), B_i^d(\rho), B_i^u(\rho), C_i^e(\rho), D_i^{ed}(\rho), D_i^{eu}(\rho)$ are satisfying

$$\begin{aligned} &A_i(\rho) = A_{i0} + A_{i1}\rho; \quad B_i^d(\rho) = B_{i0}^d + B_{i1}^d\rho; \\ &B_i^u(\rho) = B_{i0}^u + B_{i1}^u\rho; \quad C_i^e(\rho) = C_{i0}^e + C_{i1}^e\rho; \\ &D_i^{ed}(\rho) = D_{i0}^{ed} + D_{i1}^{ed}\rho; \quad D_i^{eu}(\rho) = D_{i0}^{eu} + D_{i1}^{eu}\rho. \end{aligned}$$

A controller with $u = \sum_{i=1}^{8} h_i K_i(\rho)x$ form is substituted into (11),

$$\begin{cases} \dot{x} = (A_{h\rho} + B^d_{h\rho}K_{h\rho})x + B^d_{h\rho}d, \\ e = (C^e_{h\rho} + D^{eu}_{h\rho}K_{h\rho})x + D^{ed}_{h\rho}d. \end{cases} \tag{12}$$

Full block S-procedure theorem[19] will be used twice to the quadratic terms $B^d_{h\rho}K_{h\rho}$ to lower the conservatism of 12). After completing the above work, we can successfully design a Full-State-Feedback-Controller corresponding to F-P-V-Model (8).

Theorem 2: System (12) can be controlled by the formed controller

$$u = \sum_{i=1}^{8} h_i \left(\sum_{j=0}^{1} U_{ij} P \rho_j \right) x, \tag{13}$$

if

$$\begin{bmatrix} \Pi_{2,11} + \Pi_1 & \Pi_{2,12} \\ \Pi^T_{2,12} & \Pi_{2,22} \end{bmatrix} + \tilde{M} < 0 \tag{14}$$

$$\begin{bmatrix} I_5 \\ H_i \bigotimes I_5 \end{bmatrix}^T \begin{bmatrix} \Pi_{1,11} & \Pi_{1,12} \\ \Pi^T_{1,12} & \Pi_{1,22} \end{bmatrix} \begin{bmatrix} I_5 \\ H_i \bigotimes I_5 \end{bmatrix} \geq 0 \tag{15}$$

$$\Pi_{1,22} < 0 \tag{16}$$

$$\begin{bmatrix} I_{40} \\ \rho \bigotimes I_{40} \end{bmatrix}^T \begin{bmatrix} \Pi_{2,11} & \Pi_{2,12} \\ \Pi^T_{2,12} & \Pi_{2,22} \end{bmatrix} \begin{bmatrix} I_{40} \\ \rho \bigotimes I_{40} \end{bmatrix} \geq 0 \tag{17}$$

$$\Pi_{2,22} < 0 \tag{18}$$

and

$$H = \begin{bmatrix} h_2 \\ h_3 \\ \vdots \\ h_8 \end{bmatrix}, H_1 = \begin{bmatrix} 0 \\ 0 \\ \vdots \\ 0 \end{bmatrix}, H_2 = \begin{bmatrix} 1 \\ 0 \\ \vdots \\ 0 \end{bmatrix}, \cdots, H_8 = \begin{bmatrix} 0 \\ 0 \\ \vdots \\ 1 \end{bmatrix},$$

$$\tilde{M} = \mathrm{He} \left[\begin{array}{cccccc|c} A_{10}X & B^d_{10} & 0 & \cdots & \tilde{A}_{81}X & \tilde{B}^d_{81} & 0 \\ 0 & \frac{-\gamma}{2} & 0 & \cdots & 0 & 0 & 0 \\ C^e_{10}X & D^d_{10} & \frac{-\gamma}{2} & \cdots & \tilde{C}^e_{81}X & \tilde{D}^d_{81} & 0 \\ \hline 0 & 0 & 0 & \cdots & 0 & 0 & 0 \\ \vdots & \vdots & \vdots & \vdots & \vdots & \vdots & \\ 0 & 0 & 0 & \cdots & 0 & 0 & 0 \end{array} \right]$$

$$+\mathrm{He} \begin{bmatrix} B^u_{10}U_{10} & 0 & 0 & \cdots & B^u_{10}\tilde{U}_{81} & 0 & 0 \\ 0 & 0 & 0 & \cdots & 0 & 0 & 0 \\ D^u_{10}U_{10} & 0 & 0 & \cdots & D^u_{10}\tilde{U}_{81} & 0 & 0 \\ \vdots & \vdots & \vdots & \vdots & \vdots & \vdots & \\ \tilde{B}^u_{81}U_{10} & 0 & 0 & \cdots & \tilde{B}^u_{81}\tilde{U}_{81} & 0 & 0 \\ 0 & 0 & 0 & \cdots & 0 & 0 & 0 \\ \tilde{D}^u_{81}U_{10} & 0 & 0 & \cdots & \tilde{D}^u_{81}\tilde{U}_{81} & 0 & 0 \end{bmatrix}$$

This approach allows for the adaptation of the controllers parameters to the changing dynamics of the system, enhancing its effectiveness in real-world applications.

B Dynamical-Output-Feedback-Controller

We must consider the actual working situation and reality of the probe. The detector is affected by many uncertain factors in its working process, which are often difficult for human beings to predict in advance, so the dynamic adjustment of the detector is of great practical significance. In this section, we will try to apply the dynamic output feedback controller to the model.

We consider this form of system and controller:

$$\begin{cases} \dot{x} = A_{h\rho}x + B^d_{h\rho}d + B^u_{h\rho}u, \\ e = C^e_{h\rho}x + D^{ed}_{h\rho}d + D^{eu}_{h\rho}u, \\ y = C^y_{h\rho}x + D^{yd}_{h\rho}d, \end{cases} \tag{19}$$

$$\begin{cases} \dot{x_c} = A_c x_c + B_c y, \\ u = C_c x_c + D_c y. \end{cases} \tag{20}$$

With the help of the Bounded-Real Lemma[20], we can get a controller that adapts to this model.

Theorem 3: System (19) can be controlled by(20) if the following conditions can be satisfied.

$$\begin{bmatrix} \Pi_{2,11} + \Pi_1 & \Pi_{2,12} \\ \Pi^T_{2,12} & \Pi_{2,22} \end{bmatrix} + \hat{M} < 0 \tag{21}$$

$$\begin{bmatrix} I_8 \\ H_i \bigotimes I_8 \end{bmatrix}^T \begin{bmatrix} \Pi_{1,11} & \Pi_{1,12} \\ \Pi^T_{1,12} & \Pi_{1,22} \end{bmatrix} \begin{bmatrix} I_8 \\ H_i \bigotimes I_8 \end{bmatrix} \geq 0 \tag{22}$$

$$\Pi_{1,22} < 0 \tag{23}$$

$$\begin{bmatrix} I_{64} \\ \rho \bigotimes I_{64} \end{bmatrix}^T \begin{bmatrix} \Pi_{2,11} & \Pi_{2,12} \\ \Pi^T_{2,12} & \Pi_{2,22} \end{bmatrix} \begin{bmatrix} I_{64} \\ \rho \bigotimes I_{64} \end{bmatrix} \geq 0 \tag{24}$$

$$\Pi_{2,22} < 0 \tag{25}$$

$$\begin{bmatrix} X & I_3 \\ I_3 & Y \end{bmatrix} > 0 \tag{26}$$

and

$$\hat{M} = \mathrm{He} \begin{bmatrix} A_{10}X & A_{10} & B^d_{10} & 0 & \cdots & \tilde{A}_{81}X & \tilde{A}_{81} & \tilde{B}^d_{81} & 0 \\ 0 & YA_{10} & YB^d_{10} & 0 & \cdots & 0 & Y\tilde{A}_{81} & Y\tilde{B}^d_{81} & 0 \\ 0 & 0 & \frac{-\gamma}{2} & 0 & \cdots & 0 & 0 & 0 & 0 \\ C^e_{10}X & C^e_{10} & D^{ed}_{10} & \frac{-\gamma}{2} & \cdots & \tilde{C}^e_{81}X & \tilde{C}^e_{81} & \tilde{D}^{ed}_{81} & 0 \\ 0 & 0 & 0 & 0 & \cdots & 0 & 0 & 0 & 0 \\ \vdots & \vdots & \vdots & \vdots & \vdots & \vdots & \vdots & \vdots & \\ 0 & 0 & 0 & 0 & \cdots & 0 & 0 & 0 & 0 \end{bmatrix}$$

TABLE II
SIMULATION PARAMETERS

C^*	1.34	D^*	0.32
s	$18.9\mathrm{m}^2$	m	2920kg
g	$3.71\mathrm{m/s}^2$		

$$+\mathrm{He}\begin{bmatrix} B_{10}^{u}\hat{C}_{10}^{c} & B_{10}^{u}\hat{D}^{c}C_{10}^{y} & B_{10}^{u}\hat{D}^{c}D_{10}^{yd} & 0\cdots \\ \hat{A}_{1100}^{c} & \hat{B}_{10}^{c}\hat{C}_{10}^{y} & \hat{B}_{10}^{c}\hat{C}_{10}^{yd} & 0\cdots \\ 0 & 0 & 0 & 0\cdots \\ D_{10}^{eu}\hat{C}_{10}^{c} & D_{10}^{eu}\hat{D}^{c}C_{10}^{y} & D_{10}^{eu}\hat{D}^{c}D_{10}^{yd} & 0\cdots \\ \vdots & \vdots & \vdots & \vdots\ \vdots \\ \tilde{B}_{81}^{u}\hat{C}_{10}^{c} & \tilde{B}_{81}^{u}\hat{D}^{c}C_{10}^{y} & \tilde{B}_{81}^{u}\hat{D}^{c}D_{10}^{yd} & 0\cdots \\ \hat{A}_{8110}^{c} & \hat{B}_{81}^{c}C_{10}^{y} & \hat{B}_{81}^{c}D_{10}^{yd} & 0\cdots \\ 0 & 0 & 0 & 0\cdots \\ D_{81}^{eu}\hat{C}_{10}^{c} & \tilde{D}_{81}^{eu}\hat{D}^{c}C_{10}^{y} & \tilde{D}_{81}^{eu}\hat{D}^{c}D_{10}^{yd} & 0\cdots \end{bmatrix}$$

$$\begin{bmatrix} B_{10}^{u}\hat{C}_{81}^{c} & B_{10}^{u}\hat{D}^{c}\tilde{C}_{81}^{y} & B_{10}^{u}\hat{D}^{c}\tilde{D}_{81}^{yd} & 0 \\ \hat{A}_{1801}^{c} & \hat{B}_{10}^{c}\tilde{C}_{81}^{y} & \hat{B}_{10}^{c}\tilde{D}_{81}^{yd} & 0 \\ 0 & 0 & 0 & 0 \\ D_{10}^{eu}\hat{C}_{81}^{c} & D_{10}^{eu}\hat{D}^{c}\tilde{C}_{81}^{y} & D_{10}^{eu}\hat{D}_{81}^{c}\tilde{D}_{81}^{yd} & 0 \\ \vdots & \vdots & \vdots & \vdots \\ \tilde{B}_{81}^{u}\hat{C}_{81}^{c} & \tilde{B}_{81}^{u}\hat{D}^{c}\tilde{C}_{81}^{y} & \tilde{B}_{81}^{u}\hat{D}^{c}\tilde{D}_{81}^{yd} & 0 \\ \hat{A}_{8811}^{c} & \hat{B}_{81}^{c}\tilde{C}_{81}^{y} & \hat{B}_{81}^{c}\tilde{D}_{81}^{yd} & 0 \\ 0 & 0 & 0 & 0 \\ \tilde{D}_{81}^{eu}\hat{C}_{81}^{c} & \tilde{D}_{81}^{eu}\hat{D}^{c}\tilde{C}_{81}^{y} & \tilde{D}_{81}^{eu}\hat{D}^{c}\tilde{D}_{81}^{yd} & 0 \end{bmatrix}$$

We obtained the gain-matrix by:

$$\begin{cases} A_c = N^{-1}[\hat{A}^c - Y(A_{h\rho} + B_{h\rho}D_cC_{h\rho}^{y})X - NB_cC_{h\rho}^{y}X \\ \qquad - YB_{h\rho}C_cM^T]M^{-T}, \\ B_c = N^{-1}(\hat{B}^c - YB_{h\rho}^{u}D_c), \\ C_c = (\hat{C}^c - D_cC_{h\rho}^{y}X)M^{-T}, \\ D_c = \hat{D}_c, \\ MN^T = I - XY. \end{cases} \tag{27}$$

Compared with Full-State-Feedback-Controller, this controller can be adjusted on-line in real time, which is of practical significance in the Mars exploration task with relative lack of information.

V. SIMULATION

The partial coefficient matrices of system (11) and the system (19) can be found in the appendix. When combined with the reference data provided in Fig.5 and Fig.6, and utilizing convex optimization theory, it becomes evident that there are two boundary values of density in Theorem 1, namely $0\mathrm{kg/m}^3$ and $0.4\mathrm{kg/m}^3$, respectively. Consequently, formula (10) contains 16 linear matrix inequalities, which is more easier to calculated.

A Simulation of F-S-F-Controller

We use MATLAB to solve the numerical solution of inequalities (14) ∼(18), and the results are as follows.

$$U_{10} = \begin{bmatrix} 0.0805 \\ 0.0344 \\ 0 \end{bmatrix}, U_{20} = \begin{bmatrix} 0 \\ -0.0148 \\ 0 \end{bmatrix}, U_{30} = \begin{bmatrix} 0 \\ 0 \\ 0 \end{bmatrix},$$

$$U_{40} = \begin{bmatrix} 0.1451 \\ 0 \\ 0 \end{bmatrix}, U_{50} = \begin{bmatrix} 0 \\ 0.0005041 \\ 0 \end{bmatrix}, U_{60} = \begin{bmatrix} 0.1987 \\ 0 \\ 0 \end{bmatrix},$$

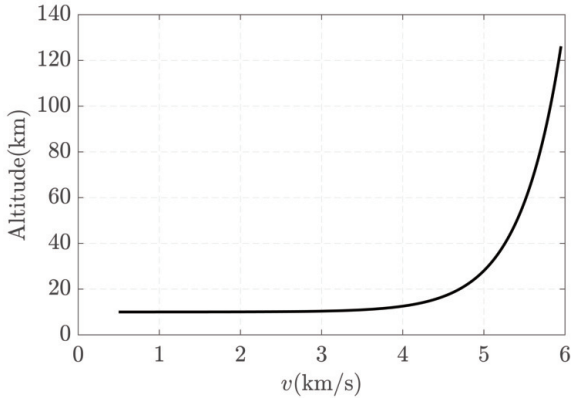

Fig. 5. Reference Trajectory

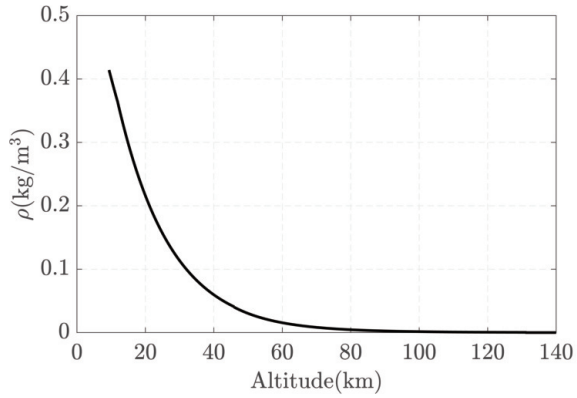

Fig. 6. Atmospheric Density

$$U_{70} = \begin{bmatrix} 0.2262 \\ -0.0141 \\ 0 \end{bmatrix}, U_{80} = \begin{bmatrix} 0.1347 \\ 0.0107 \\ 0 \end{bmatrix}, U_{11} = \begin{bmatrix} 0 \\ -0.0001103 \\ 0 \end{bmatrix},$$

$$U_{21} = \begin{bmatrix} -0.0355 \\ 0 \\ 0 \end{bmatrix}, U_{31} = \begin{bmatrix} -2.4307 \\ -0.0004 \\ 0 \end{bmatrix}, U_{41} = \begin{bmatrix} 0.0077 \\ -0.0037 \\ 0 \end{bmatrix},$$

$$U_{51} = \begin{bmatrix} 0 \\ 0.0035 \\ 0 \end{bmatrix}, U_{61} = \begin{bmatrix} 0 \\ 0 \\ 0 \end{bmatrix}, U_{71} = \begin{bmatrix} -1.6878 \\ 0 \\ 0 \end{bmatrix},$$

$$U_{81} = \begin{bmatrix} 0 \\ -0.0009045 \\ 0 \end{bmatrix},$$

$$P = \begin{bmatrix} 1.5020 & -0.1100 & -0.2568 \\ -0.1100 & 10.9836 & 6.1894 \\ -0.2568 & 6.1894 & 9.6415 \end{bmatrix}.$$

Substituting the solved controller (13) into system (12), the results shown in Fig.7 and Fig.8 can be obtained. From the figure, we can see that under the control of the F-S-F-Controller, the detector can reach the parachute opening height in three minutes, and at the same time reduce the speed to about 400 meters per second. This simulation result is reasonable and provides a good prerequisite for the next phase of the task.

B Simulation of D-O-F-Controller

Solving the numerical solution of inequalities (21) ∼ (26) and controller (20) will be received. Substituting the solved

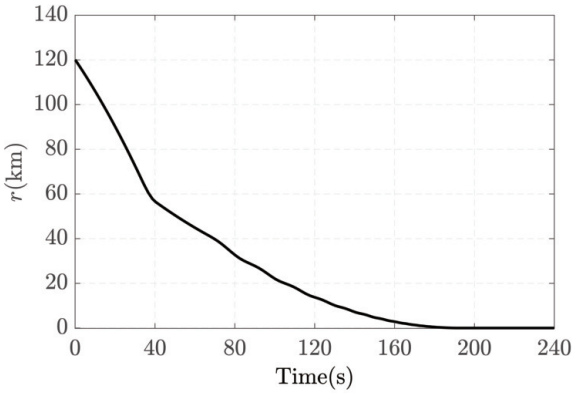

Fig. 7. r of (12) Under F-S-F-Controller

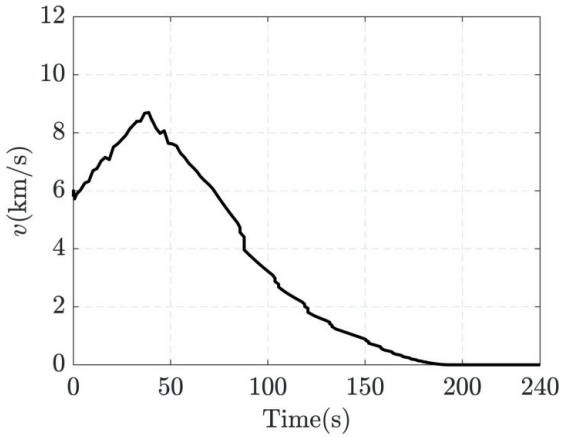

Fig. 8. v of (12) Under F-S-F-Controller

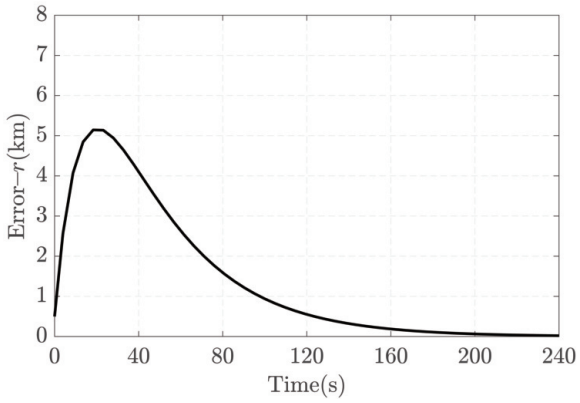

Fig. 9. Error of Altitude

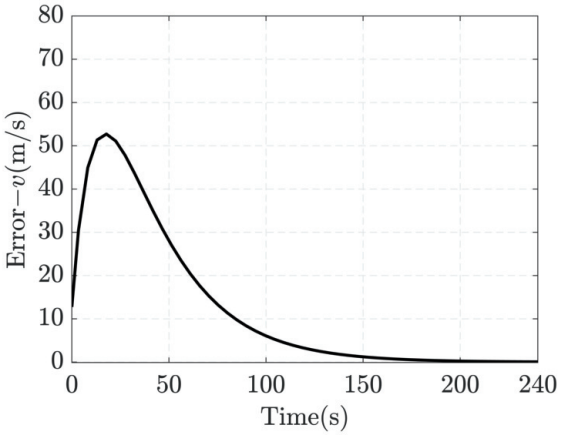

Fig. 10. Error of Speed

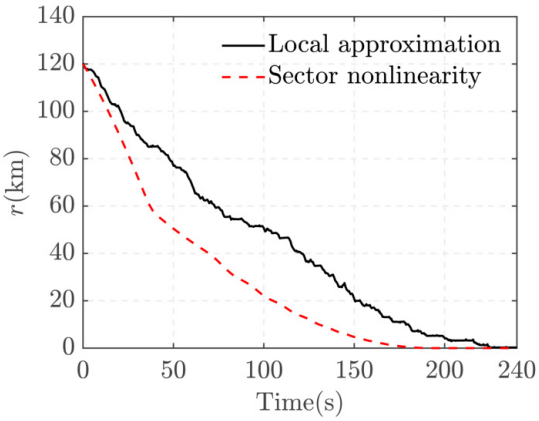

Fig. 11. A Simulation Comparison between the Two Methods-r

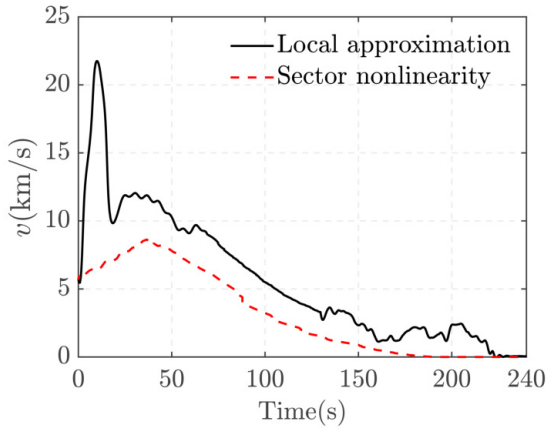

Fig. 12. A Simulation Comparison between the Two Methods-v

controller into system (19) to track the reference trajectory given in Fig.5.

Fig.9 and Fig.10 show the error between the actual working condition of the detector and the set target under the dynamic output feedback controller. Although the detector deviates from the trajectory in the first 20 seconds, it can be adjusted within 1 minute and basically coincides with the set trajectory after 2 minutes. It is clearly that under the control of the dynamic output feedback controller, the detector can be adjusted in real time and fit the set trajectory infinitely.

C Comparative Analysis

Local approximation is a method to deal with nonlinear systems. In this chapter, we will compare the model advantages of the two methods. This comparison will provide insights into the effectiveness and performance of the different modeling techniques, guiding future applications in similar contexts.

From Fig.11 and Fig.12, it is evident that the model constructed by sector nonlinearity enables smoother landing in a shorter time, with significantly reduced speed fluctu-

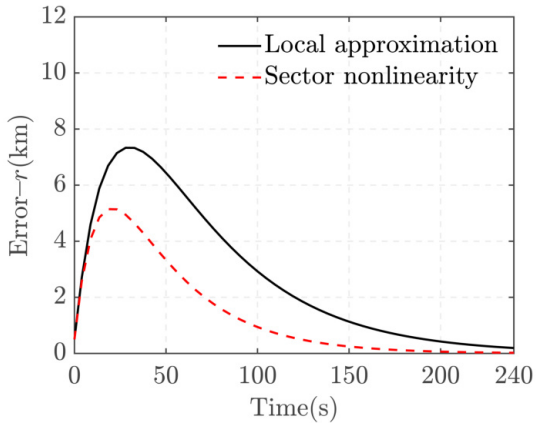

Fig. 13. Error Analysis-r

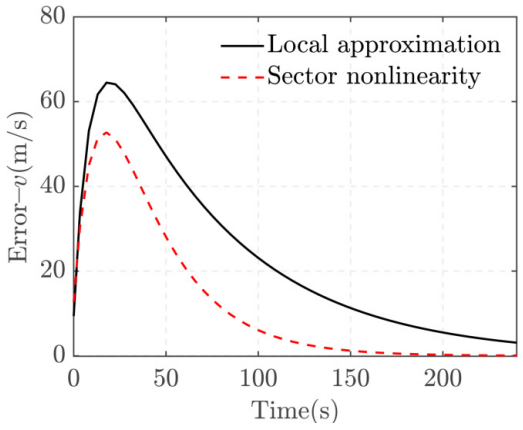

Fig. 14. Error Analysis-v

ations during the process, compared to the local approximation. Additionally, in the case of the D-O-F-Controller, it is observed from Fig.13 and Fig.14 that the error is smaller. These findings highlight the superior performance and effectiveness of the controllers designed using sector nonlinearity, demonstrating their potential to enhance the precision and reliability of the landing process for the Mars rover.

APPENDIX A
COEFFICIENT MATRICES OF THE SYSTEM (11) AND THE SYSTEM (19)

$$A_{10}=\begin{bmatrix}0 & 7.6371\times10^{-2} & 0\\ 0 & 0 & -10\\ -1.9500\times10^{-1} & 0 & 0\end{bmatrix},$$

$$A_{11}=\begin{bmatrix}0 & 0 & 0\\ 0 & -5.8445\times10^{-4} & 0\\ 0 & 0 & 0\end{bmatrix},$$

$$A_{20}=\begin{bmatrix}0 & 7.6371\times10^{-2} & 0\\ 0 & 0 & -1\\ -9.9978\times10^{-4} & 0 & 0\end{bmatrix},$$

$$A_{21}=\begin{bmatrix}0 & 0 & 0\\ 0 & -6.8965\times10^{-3} & 0\\ 0 & 0 & 0\end{bmatrix},$$

$$A_{30}=\begin{bmatrix}0 & 7.6371\times10^{-2} & 0\\ 0 & 0 & -9.9903\times10^{-1}\\ -1.9500\times10^{-1} & 0 & 0\end{bmatrix},$$

$$A_{31}=\begin{bmatrix}0 & 0 & 0\\ 0 & -5.8445\times10^{-4} & 0\\ 0 & 0 & 0\end{bmatrix},$$

$$A_{40}=\begin{bmatrix}0 & 7.6371\times10^{-2} & 0\\ 0 & 0 & -9.9903\times10^{-1}\\ -9.9978\times10^{-4} & 0 & 0\end{bmatrix},$$

$$A_{41}=\begin{bmatrix}0 & 0 & 0\\ 0 & -6.8965\times10^{-3} & 0\\ 0 & 0 & 0\end{bmatrix},$$

$$A_{50}=\begin{bmatrix}0 & -7.6371\times10^{-2} & 0\\ 0 & 0 & -1\\ -1.9500\times10^{-1} & 0 & 0\end{bmatrix},$$

$$A_{51}=\begin{bmatrix}0 & 0 & 0\\ 0 & -5.8445\times10^{-4} & 0\\ 0 & 0 & 0\end{bmatrix},$$

$$A_{60}=\begin{bmatrix}0 & -7.6371\times10^{-2} & 0\\ 0 & 0 & -1\\ -9.9978\times10^{-4} & 0 & 0\end{bmatrix},$$

$$A_{61}=\begin{bmatrix}0 & 0 & 0\\ 0 & -6.8965\times10^{-3} & 0\\ 0 & 0 & 0\end{bmatrix},$$

$$A_{70}=\begin{bmatrix}0 & -7.6371\times10^{-2} & 0\\ 0 & 0 & -9.9903\times10^{-1}\\ -1.9500\times10^{-1} & 0 & 0\end{bmatrix},$$

$$A_{71}=\begin{bmatrix}0 & 0 & 0\\ 0 & -5.8445\times10^{-4} & 0\\ 0 & 0 & 0\end{bmatrix},$$

$$A_{80}=\begin{bmatrix}0 & -7.6371\times10^{-2} & 0\\ 0 & 0 & -9.9903\times10^{-1}\\ -9.9978\times10^{-4} & 0 & 0\end{bmatrix},$$

$$A_{81}=\begin{bmatrix}0 & 0 & 0\\ 0 & -6.8965\times10^{-3} & 0\\ 0 & 0 & 0\end{bmatrix},$$

$$B_{10}^{u}=\begin{bmatrix}0\\0\\0\end{bmatrix},B_{11}^{u}=\begin{bmatrix}0\\0\\1.3957\times10^{-4}\end{bmatrix},B_{20}^{u}=\begin{bmatrix}0\\0\\0\end{bmatrix},$$

$$B_{21}^{u}=\begin{bmatrix}0\\0\\1.6469\times10^{-3}\end{bmatrix},B_{30}^{u}=\begin{bmatrix}0\\0\\0\end{bmatrix},B_{31}^{u}=\begin{bmatrix}0\\0\\1.3957\times10^{-4}\end{bmatrix},$$

$$B_{40}^{u}=\begin{bmatrix}0\\0\\0\end{bmatrix},B_{41}^{u}=\begin{bmatrix}0\\0\\1.6469\times10^{-3}\end{bmatrix},B_{50}^{u}=\begin{bmatrix}0\\0\\0\end{bmatrix},$$

$$B_{51}^{u}=\begin{bmatrix}0\\0\\1.3957\times10^{-4}\end{bmatrix},B_{60}^{u}\begin{bmatrix}0\\0\\0\end{bmatrix},B_{61}^{u}=\begin{bmatrix}0\\0\\1.6469\times10^{-3}\end{bmatrix},$$

$$B_{70}^{u}=\begin{bmatrix}0\\0\\0\end{bmatrix},B_{71}^{u}=\begin{bmatrix}0\\0\\1.3957\times10^{-4}\end{bmatrix},B_{80}^{u}=\begin{bmatrix}0\\0\\0\end{bmatrix},$$

$$B_{81}^{u}=\begin{bmatrix}0\\0\\1.6469\times10^{-3}\end{bmatrix}.$$

REFERENCES

[1] R. Braun and R. Manning, "Mars exploration entry descent and landing challenges," *Journal of Spacecraft and Rockets*, vol. 44, pp.18, 2007.

[2] S. Li and X. Jiang, "Review and prospect of guidance and control for mars atmospheric entry," *Progress in Aerospace Sciences*, vol. 69, pp. 40–57, 2014.

[3] S. L. Hess , R. M. Henry and C. B. Leovy,"Meteorological results from the surface of Mars: Viking 1 and 2," *Journal of Geophysical Research*, vol. 82, no. 28, pp. 4559-4574, 1977.

[4] W. E. Combs and J. E. Andrews, "Combinatorial rule explosion eliminated by a fuzzy rule configuration," *IEEE Transactions on fuzzy Systems*, vol. 6, no. 1, pp. 1-11, 1998.

[5] G. Ren, H. Cui, P. Cui, and E. Luan, "A rapid uncertainty propagation method for pre-parachute phase of mars entry," *2011 Chinese Control and Decision Conference (CCDC)*, 2011.

[6] T. Zhao, C. Li, and Z. Zang, "ChebyshevCLegendre pseudo-spectral method for the generalised BurgersCFisher equation," *2011 Applied Mathematical Modelling*, vol. 36, no. 3, pp. 1046-1056, 2012.

[7] X. Feng, Y. Lv, and Y. Gao, "Adaptive Radau pseudo-spectral optimization for descending trajectory of a hypersonic cruise vehicle," *Aerospace Systems*, vol. 3, pp. 275-286, 2020.

[8] Y. Liu, Y. Qian, J. Li, and C. Gao, "Mars exploring trajectory optimization using gauss pseudo-spectral method," *2012 IEEE International Conference on Mechatronics and Automation (ICMA)*, 2012.

[9] S. Li and Y. Peng, "Mars entry trajectory optimization using doc and dcnlp," *Advances in Space Research*, vol. 47, no. 3, pp. 440–452, 2011.

[10] D. Juan and Y. Xia, "Mars atmospheric entry guidance for reference trajectory tracking," *Aerospace Science and Technology*, vol. 45, pp. 335–345, 2015.

[11] J. Dai, A. Gao, and Y. Xia, "Mars atmospheric entry guidance for reference trajectory tracking based on robust nonlinear compound controller," *Acta Astronautica*, vol. 132, pp. 221–229, 2017.

[12] J. Long, S. Zhu, P. Cui, and Z. Liang, "Barrier Lyapunov function based sliding mode control for mars atmospheric entry trajectory tracking with input saturation constraint," *Aerospace Science and Technology*, vol. 106, pp. 106–213, 2020.

[13] V. Saranya, V. Chinnaponnu, M. P. Rijesh, and N. K. Philip, "Mars entry phase trajectory tracking controller using dynamic inversion," *2018 International Conference on Current Trends towards Converging Technologies (ICCTCT)*, vol. 2018, pp. 1–6, 2018.

[14] Y. Huang, S. Li, and J. Sun, "Mars entry fault-tolerant control via neural network and structure adaptive model inversion," *Advances in Space Research*, vol. 63, pp. 557–571, 2019.

[15] E. G. Collins, "Fuzzy control systems design and analysis: a linear matrix inequality approach," *Automatica*, vol. 39, pp. 2011–2013, 2003.

[16] H. Xu, H. Cui, and Y. Tian, "Comparison of two robust optimal trajectory design methods for mars entry," *ICIC Express Letters*, vol. 9, pp. 2437–2443, 2015.

[17] X. Ban, H. Zhang, and F. Wu, "Stability analysis and controller design for a novel nonlinear system: Fuzzy parameter varying system," *Journal of Intelligent and Fuzzy Systems*, vol. 34, pp. 1–9, 2018.

[18] X. Ban, H. Zhang, and F. Wu, "Stability analysis with quadratic Lyapunov functions: Some necessary and sufficient multiplier conditions," *Systems and Control Letters*, vol. 57, pp. 78-94, 2008.

[19] C. Scherer, "LPV control and full block multipliers," *Automatica*, vol. 37, pp. 361–375, 2001.

[20] H. S.Wang , C. F.Yung and F. R.Chang, "Bounded real lemma and H_∞ control for descriptor systems," *IEE Proceedings-Control Theory and Applications*, vol. 145, pp. 316-322, 1998.